

Photo-carrier and Electronic Studies of Silicon-Doped GaAs Grown by MBE Using PCR

J. A. Villada · S. Jiménez-Sandoval ·
M. López-López · J. Mendoza ·
D. G. Espinosa-Arbeláez · M. E. Rodríguez-García

Received: 28 June 2009 / Accepted: 10 May 2010 / Published online: 30 May 2010
© Springer Science+Business Media, LLC 2010

Abstract Photo-carrier radiometry (PCR) has been used to study the distribution of impurities and the lattice damage in silicon-doped gallium arsenide in a noncontact way. The results from the PCR study are correlated with Hall effect measurements. Samples for this study were grown by molecular beam epitaxy. Of all possible parameters that can be manipulated, the silicon effusion cell temperature was the only one that was varied, in order to obtain samples with different silicon concentrations. The distribution of impurities was obtained by scanning the surface of each sample. The PCR amplitude and phase images were obtained as a function of the $x-y$ position. According to the PCR images, it is evident that the impurities are not uniformly distributed across the sample. From these images, the average value of the amplitude and phase data across the surface was obtained for each sample in order to study the PCR signal behavior as a function of the silicon effusion cell temperature.

Keywords Electrical properties · Photo-carrier radiometry · Si-doped GaAs · Thermoelectronic images

J. A. Villada · S. Jiménez-Sandoval
Centro de Investigación y de Estudios Avanzados del IPN, Unidad Querétaro, Apdo. Postal 1-798,
CP 76001 Querétaro, Qro, México

M. López-López · J. Mendoza
Departamento de Física, Centro de Investigación y de Estudios Avanzados del IPN, Avenida IPN,
2508 México, DF, México

D. G. Espinosa-Arbeláez · M. E. Rodríguez-García (✉)
Departamento de Nanotecnología, Centro de Física Aplicada y Tecnología Avanzada, UNAM Campus,
Juriquilla, Querétaro, Qro, México
e-mail: mariorodga@gmail.com

1 Introduction

GaAs molecular beam epitaxial (MBE) layers are currently used in a variety of microelectronic and optoelectronic devices such as high electron mobility transistors (HEMTs) and lasers. Silicon (Si) doping is typically used in MBE growth when n-type doped layers are required in these devices. A Knudsen type effusion cell is commonly used to produce the flux of Si atoms. The cell temperature is the parameter employed to control the flux of Si atoms and therefore the doping level.

One of the main concerns in relation to any semiconductor material is the study of electronic properties. Many techniques have been implemented in order to determine the electronic properties of semiconductor materials, but all of them require manipulation of the samples and they become useless for later studies. This problem can be resolved using a noncontact technique. Moreover, the distribution of impurities in the semiconductor is an important aspect in the manufacture of integrated circuits. Photo-carrier radiometry (PCR) is a new powerful technique that has been used to obtain different electronic transport parameters such as recombination lifetime, front and back surface recombination velocities, carrier diffusion coefficient [1, 2], and the distribution of the impurities on semiconductor wafers [3]. Unlike other photothermal techniques like photothermal radiometry (PTR) or photo-modulated thermoreflectance (PMOR), PCR is only sensitive to the recombination of free photo-excited carrier density waves [1].

This article demonstrates that PCR can yield information, not only about the aforementioned electronic parameters, but also about the carrier density and the mobility. The distribution of the impurities on the surface and the carrier density of the sample are evaluated in a contactless, noninvasive, and nondestructive manner. Si-doped GaAs layers with different Si concentrations grown using molecular beam epitaxy were studied using PCR. The results are correlated with Hall effect measurements.

2 Sample Description

Semi-insulator undoped GaAs (100) wafers from Atramat Inc., USA with a resistivity of $10^8 \Omega \cdot \text{cm}^{-1}$, and an etch pit density (EPD) of less than 10^3 cm^{-2} with both sides polished, 50.8 mm in diameter and 400 μm thick (epi-ready), were used for this study as substrates to grow a set of seven samples of Si-doped GaAs. The samples were grown in a Riber C21 MBE system. The temperature of the Si effusion cell was varied from 1120 °C to 1300 °C in order to obtain GaAs layers with different Si concentrations. Table 1 shows the temperature of the Si effusion cell for each sample in the study. The final carrier concentration and the mobility were obtained by Hall measurements at room temperature. Parameters such as substrate temperature, Gallium effusion cell temperature, and growth time remained constant. The temperature of the doping (Si) effusion cell was the only parameter that was varied.

Table 1 Temperature of the Si effusion cell for each sample in the study

Sample	T_{Si} (°C)
44	1300
45	1270
46	1240
64	1200
65	1180
66	1140
67	1120

3 Measuring Methods

3.1 Hall Measurements

For Hall measurements metal contacts of indium were deposited on the samples. The samples were then annealed in a N₂ atmosphere at 450 °C for 30 s. The samples were then bonded using indium pellets and gold wires. The current–voltage characteristics exhibited ohmic behavior at room temperature and 77 K. Hall effect measurements were carried out at room temperature in a conventional system.

3.2 PCR Measurements

The photo-carrier radiometric system is schematically shown in Fig. 1. A 532 nm solid-state laser was used as an excitation source. After focusing, the laser beam diameter on the sample was 40 μm. The intensity modulated laser beam impinging on the GaAs surface produces simultaneously direct heating due to absorption, as well as a modulation of the free photo-excited carrier density. For GaAs, excited carriers can diffuse several tens of μm's before recombination. According to the diffusion laws, they are moving away from the excitation region. If the IR emissions from the recombination region of the sample are filtered and focused onto a narrow-bandwidth IR detector, such as InGaAs which has a spectral bandwidth from 800 nm to 1800 nm, a PCR signal free of any thermal contribution can be obtained [1]. The diameter of the detecting area focused in our system is similar to the excitation area, about 40 μm. The resulting IR radiation is primarily due to the optical recombination of photo-excited carriers, and the signal can be expressed in the form as follows:

$$s(\omega) = F(\lambda_1, \lambda_2) \int_0^L \Delta N(z, \omega) dz \quad (1)$$

where $F(\lambda_1, \lambda_2)$ is a coefficient related to the detector bandwidth [λ_1, λ_2], $\Delta N(z, \omega)$ is the carrier-wave depth profile, z is the depth starting from the sample wafer front surface, and ω is the angular frequency of the modulated excitation beam. Frequency

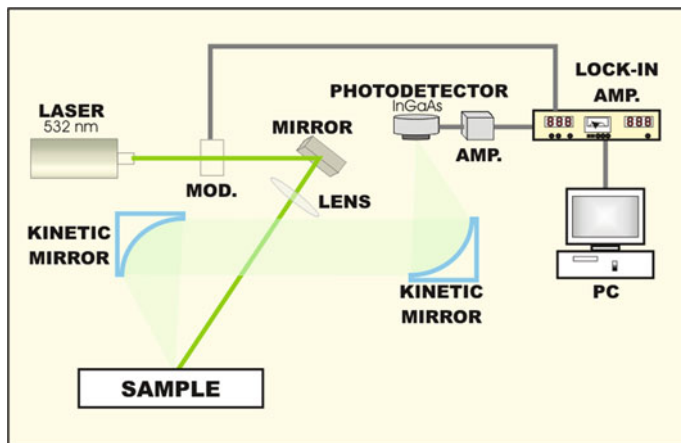


Fig. 1 Schematic of the PCR system

scans were carried out in order to determine the optimal frequency. A frequency of 4170 Hz was chosen for all measurements. The PCR signal is directly proportional to the depth integral of the carrier density in the sample; therefore, it is sensitive to lattice damage induced by processes such as ion implantation and impurities.

The excitation source used for PCR measurements has a greater energy than the gap energy of the material (1.42 eV at room temperature); therefore, all the impurities are excited and, in the relaxation process, they all contribute to the PCR signal which is limited only by the bandwidth of the detector (0.69 eV to 1.55 eV). On the other hand, when the concentration of impurities is high, structural damage is substantial.

4 Results

Before discussing the results, it is necessary to show the direct relation between the Si effusion cell temperature and the Si concentration in the sample. The MBE system used in the growth of the samples employ Knudsen effusion cells for the atom beam generation of gallium, arsenic, and Si. The arrival rate of the atoms at the substrate surface can be calculated from thermodynamic parameters of the cell as shown in Knudsen [4]

$$j = (K) \frac{nA\sqrt{T}}{Vl^2\sqrt{M}} \text{ molecules cm}^{-2} \cdot \text{s}^{-1} \quad (2)$$

where j is the atom flux to the substrate, K is a constant, n is the number of particles into the cell, A is the area of the output orifice, T is the cell temperature in K, V is the cell volume, l is the distance from the substrate, and M is the molar mass of the source material. In general, not all of the atoms arriving on the surface are incorporated on it; some of them are re-evaporated; therefore, the atom incorporation rate into the sample is given as

$$R = \alpha j \quad (3)$$

where α is the sticking coefficient. From Eqs. 2 and 3 it is clear that for high temperatures values in the impurity (Si) effusion cell, the concentration of the impurities in the sample will be proportionately high.

Si is incorporated into the material forming different kinds of defects. Three of the more important of these are explained as follows: due to the amphoteric behavior of the atoms of group IV, Si can occupy both the arsenic (Si_{As}) and gallium (Si_{Ga}) lattice sites exhibiting acceptor and donor properties, respectively. In addition, the coulomb interaction between two kinds of defects, namely, gallium vacancies (V_{Ga}) and Si_{Ga} , produces a third kind of acceptor defect called a dopant–vacancy complex ($\text{Si}_{\text{Ga}}-\text{V}_{\text{Ga}}$).

For Si-doped GaAs (n-type) it is well known that for high Si concentrations (higher than 10^{19} cm^{-3}), an electrical deactivation process occurs [5, 6]. This phenomenon can be explained because the density of the two kinds of acceptor defects ($\text{Si}_{\text{Ga}}-\text{V}_{\text{Ga}}$ and Si_{As}) increases with the Si concentration [7, 8]. These defects compensate for the electrical effect of the n-type Si_{Ga} impurities.

Figure 2 shows the transport parameters as measured by the Hall effect as a function of the Si effusion cell temperature. Figure 2a shows the n-type carrier concentration; the aforementioned electrical deactivation phenomenon can be observed in this figure for temperatures higher than 1230 °C. According to Domke et al. [7], at temperatures lower than 1230 °C predominance of n-type Si_{Ga} defects exists, but for higher temperatures the concentration of the p-type $\text{Si}_{\text{Ga}}-\text{V}_{\text{Ga}}$ and Si_{As} defects increase drastically; therefore, the n-type electrical behavior decreases and the damage in the lattice increases. In Fig. 2b the effect in the mobility of the sample can be seen when the Si concentration increases. The mobility of the carrier decreases due to the lattice damage produced at high Si concentrations.

The PCR analysis is divided into two parts: the analysis of one sample as a function of the position (homogeneity) and the analysis for all samples as a function of the Si effusion cell temperature.

4.1 Sample Homogeneity

Due to the high sensitivity to photo-carrier emission, PCR signal scans on the surface can provide information about the distribution of impurities and the lattice damage across the sample. Images of both the phase and amplitude are shown in Fig. 3a and b, respectively, for the surface of sample 44 (1300 °C) taken at 4170 Hz. This sample was chosen because it has the highest PCR intensity as will be demonstrated in the next section. In this image it is clear that the intensity and phase are not the same for the whole surface. Because PCR is sensitive only to the photo-carrier emission, it is possible to conclude that the distribution of the impurities is non-homogeneous. This behavior could be the result of the geometry of the MBE chamber.

By comparing the phase and amplitude shown in Fig. 3, it is possible to see that in zones with high PCR amplitude ($x = 0, y = 0$) the phase exhibits low values that could be associated to a low diffusion coefficient of the excited photo-carriers. Lattice

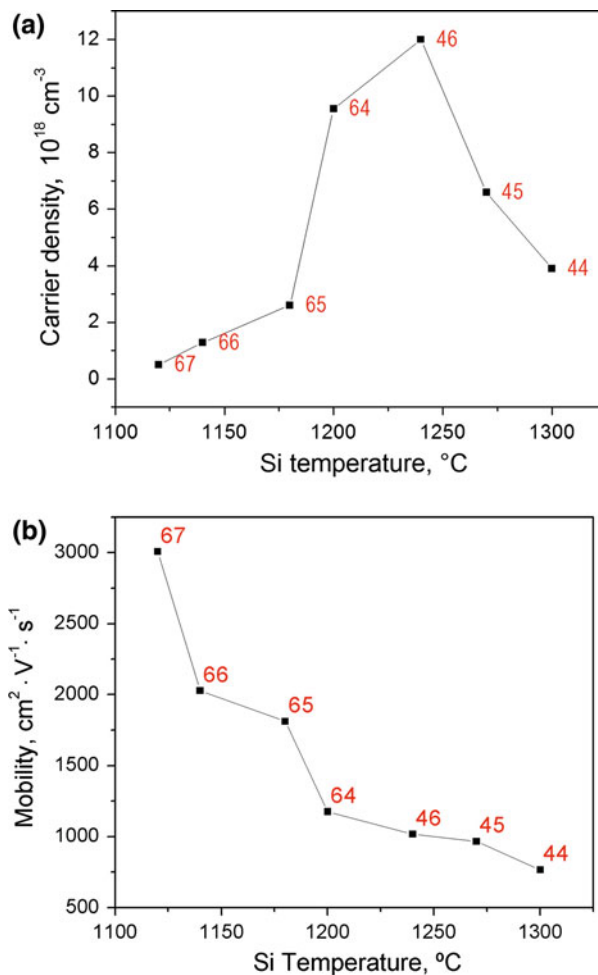


Fig. 2 Transport parameters measured by Hall effect as a function of the Si effusion cell temperature: (a) carrier density and (b) mobility

damage produced by the high Si concentration reduces the diffusion, and consequently, the mobility of the carriers.

4.2 PCR Signal as a Function of the Si Effusion Cell Temperature

Similar images were taken for each sample, and all values were averaged in order to obtain a unique value for the PCR amplitude and the phase signal with the respective standard deviation per point. Figure 4 shows these values for each sample. Figure 4a shows the amplitude of the PCR signal as a function of the Si effusion cell temperature. Assuming that the PCR signal is proportional to the excited photo-carriers, the effect of the electrical deactivation cannot be observed in this figure because all impurities,

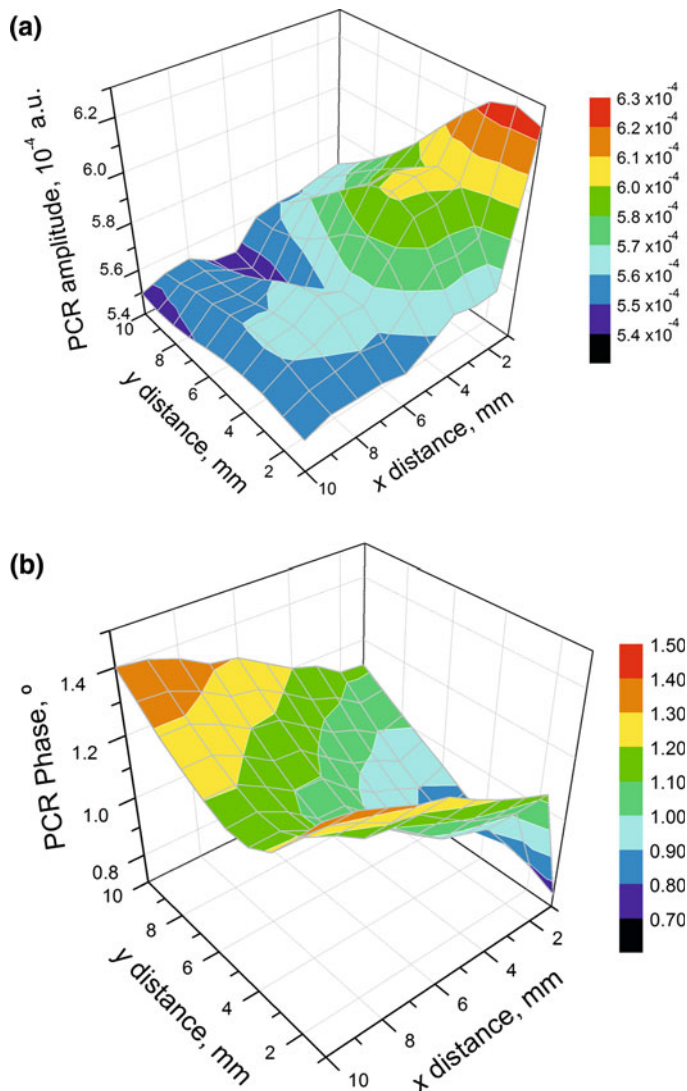


Fig. 3 PCR images of GaAs sample 44: (a) amplitude and (b) phase

n-type and p-type, contribute to increasing the PCR signal. On the other hand, the PCR amplitude is related with the carrier mobility as follows: at low Si concentration, the crystalline quality is only slightly affected, and the mobility is high enough such that carriers can diffuse and recombine outside of the detection area. Therefore, the system only detects the carrier diffusing in the z direction. For this reason at low Si effusion cell temperatures, the PCR amplitude is constant. For Si effusion cell temperatures higher than 1180°C , the crystalline quality decreases and, consequently, the mobility decreases as well. Therefore, carriers can recombine into the detection area and the PCR amplitude increases. Above this temperature, the increase in the Si concentration

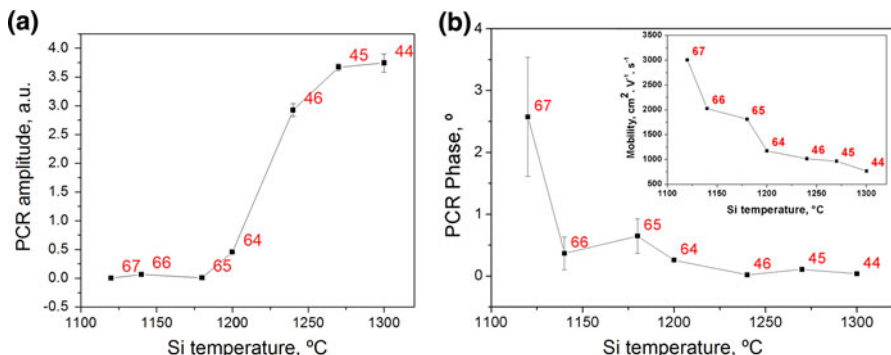


Fig. 4 Average of the (a) amplitude and (b) phase from the PCR images like those shown in Fig. 3 for all samples

produces an increase in the PCR signal. However, for higher Si concentrations, the emissivity of the sample decreases due to the high lattice damage. Therefore, the slope of the curve in Fig. 4a is reduced at high Si effusion cell temperatures.

The average of the PCR phase for all samples is shown in Fig. 4b. The effect of the lattice damage can be observed in this figure, now in correlation with the Si concentration. For samples with high Si concentrations, the mobility decreases and a rapid PCR response is obtained; therefore, the PCR phase decreases. The inset in Fig. 4b corresponds to Fig. 2b which was included here to show the similar behavior of both the carrier mobility and the PCR phase.

5 Conclusions

This is the first time the PCR technique has been used to obtain information about the carrier distribution and the lattice damage in silicon-doped GaAs. In samples grown using MBE, the Si is not distributed uniformly in the material. A direct correlation between the PCR phase and the carrier mobility exists because both parameters are related to the lattice damage caused by the drastic increase in the Si_{As} and $\text{Si}_{\text{Ga}}-\text{V}_{\text{Ga}}$ defects at high Si concentrations. While both of these defects compensate the n-type electrical behavior of a sample, in the PCR signal all of them contribute to the PCR amplitude. For this reason, at a high Si concentration, the PCR amplitude is high.

Acknowledgments This work was partially supported by Project No. PAPIIT IN120809 2009/11, Universidad Nacional Autónoma de México, CONACYT-México, and ICTDF. The authors would like to thank R. Fragoso and E. Gomez for technical assistance. J. A. Villada and D. G. Espinosa would also like to thank CONACYT for the financial support for PhD studies. The authors would like to thank Silvia C. Stroet of the Engineering Faculty at UAQ University for her technical support in editing the English of this article.

References

1. A. Mandelis, J. Batista, D. Shaughnessy, Phys. Rev. B **67**, 205208 (2003)
2. A. Mandelis, NDT&E Int. **39**, 244 (2006)

3. R. Velázquez-Hernández, J. García-Rivera, M.E. Rodriguez-Garcia, S. Jiménez-Sandoval, J.A. Mendoza-Álvarez, J.G. García, J. Appl. Phys. **101**, 023105 (2007)
4. M. Knudsen, Ann. Phys. (Leipzig) **4**, 999 (1909)
5. K. Ploog, A. Fischer, H. Kunzel, J. Electrochem. Soc. **128**, 400 (1981)
6. Y.G. Chai, R. Chow, C.E.C. Wood, Appl. Phys. Lett. **39**, 800 (1981)
7. C. Domke, Ph. Ebert, M. Heinrich, K. Urban, Phys. Rev. B **54**, 10228 (1996)
8. S. Modesti, R. Duca, P. Finetti, G. Ceballos, M. Piccin, S. Rubini, A. Franciosi, Phys. Rev. Lett. **92**, 086104-1 (2004)